Supplementary Information N°1 for

Development of an Analytical Model of Automobile Energy Consumption During Use-Phase for Parametrized Life Cycle Assessment

Gabriel Magnaval [1,*], Anne-Marie Boulay [1]

[1] CIRAIG, Department of Chemical Engineering, Polytechnique Montreal, 2500 Chem. De Polytechnique, Montreal, Canada

[*] corresponding author details: gabriel.magnaval@polymtl.ca

Aim of this document

This document gathers all detailed calculation for obtaining the parametrized equations to calculate energy consumption of GV and BEV. It is divided into three sections. The first section is an overview which presents the main equations of the model. The second section focuses on the energy consumption assumptions and equations (external forces, powertrain losses, ect.). The third section presents the integration model, with all assumptions and detailed calculations.

Table of content

1- Overview of the model

1.1- Physical Drivers included in the power demand modelling

*Table S1: Raw equations used in the methodology to parametrize **power demand** of automobile.*

Driver	Equation	Other source
A- External Forces		
Rolling	$P_{rolling} = r_0 Mgvcos\theta \approx r_0 Mgv$	1–5
Aerodynamic drag	$P_{aero} = 0.5\, \rho C_D A v^3$	1–5
Inertia	$P_{inertia} = M \frac{dv}{dt} v$	1–5
Rotating inertia	$P_{rotating} = 4 \frac{I_w}{{r_w}^2} \frac{dv}{dt} v$	1–3
Grade	$P_{grade} = Mgvsin\theta$	3–5
Additional drag due to wind	$P_{wind} = 0.5\, \rho C_D A v v_{wind}^2$	6–8
$\boldsymbol{r_0}$ [-] rolling factor; **M** [kg] vehicle weight; **v** [m/s] vehicle speed; $\boldsymbol{\rho}$ [-] air density; $\boldsymbol{C_d}$ [-] drag coefficient; **A** [m²] vehicle frontal area; $\boldsymbol{I_w}$ [] polar moment of the inertia of the wheels; $\boldsymbol{r_w}$ [m] effective radius of the wheels; $\boldsymbol{\theta}$ [rad] road slope; $\boldsymbol{v_{wind}}$ [m/s] : wind speed		
B- Gasoline Engines Losses		
Thermodynamic	$P_{thermo} = \frac{1}{{r_c}^{\gamma-1}} P_{in,GV}$	1,4,9
Frictions	$P_{fr} = \frac{fmep_0 DN}{4\pi} - mP_{in,GV}$	4,10,11
Thermal	$P_{th} = (Q_0 D + qP_{in,GV})$	4,12
Injection	$P_{inj} = \phi_{FA} P_{in}$	1,4
Pumping	$P_{pump} = \frac{p_0 DN^3}{4\pi}$	4,13,14
Cold Start	$E_{cs} = c_s P_e$	15
$\boldsymbol{P_{in}}$ [W] power demand; $\boldsymbol{N}$ [rad/s] engine speed; **T** [N] engine torque; $\boldsymbol{r_c}$ [-] compression ratio; $\boldsymbol{\gamma}$ [-] heat capacity ratio; $\boldsymbol{fmep_0}$ [kPa] friction mean pressure at no load; **D** [L] engine displacement; **m** [-] effective manifold intake loss; $\boldsymbol{Q_0}$ [kPa/s] insulation losses at no load; **q** [-] effective combustion losses; $\boldsymbol{\phi_{FA}}$ [-] fuel-air ratio loss; $\boldsymbol{p_0}$ [kPa.s2] pumping mean effect at no load; $\boldsymbol{c_s}$ [J/W/m] cold start constant; $\boldsymbol{P_e}$ [W] maximum power of the engine.		
C- Electric Engines Losses		
Core	$P_{core} = \delta P_{in,BEV}$	16,17
Conductive	$P_{cop} = \varepsilon T^2$	
Converter	$P_{other} = \beta$	
Friction	$P_{other} = \alpha N$	
$\boldsymbol{P_{in}}$ [W] power demand; $\boldsymbol{N}$ [rad/s] engine speed; **T** [N] engine torque; $\boldsymbol{\alpha\ [J], \beta[W], \delta[-], \varepsilon[s.kg^{-1}]}$ electric engine characteristic constant.		
D- Drivetrain Losses		
Frictions	$P_{trans} = (a_{tr} P_e N + cP_{in,dr})$	18–20
Synchronization	$E_{synchro} = S.d$	
$\boldsymbol{P_{in}}$ [W] power demand; $\boldsymbol{N}$ [rad/s] engine speed; $\boldsymbol{P_e}$ [W] maximum power of the engine; $\boldsymbol{a_{tr}}$ [s], **c** [-] drivetrain characteristic constant; **S** [J/m] synchronization loss constant; **d** [m] distance traveled.		
E- Battery Losses		
Charging	$P_{charging} = (1 - \eta_{charging}) P_{in,charg}$	21–24

Discharging		$P_{discharging} = R(\frac{P_{in,bat}}{U})^2$	
$\boldsymbol{P_{in}}$ [W] power demand; $\boldsymbol{\eta_{charg}}$ [-] battery charging efficiency; **R** [ohm] internal resistance of the battery; **U** [V] battery voltage.			
F- Regenerative Braking			
Regen.		$P_{regen} = \left(\frac{(2B - B_{lim})^2}{4B^2}\right) P_{inertia}$	25,26
$\boldsymbol{P_{inertia}}$ [W] power demand for inertia; **B** [m/s²] mean deceleration during braking; $\boldsymbol{B_{lim}}$ [m/s²] safety limit of regenerative braking deceleration.			
G- Accessories Losses			
Accessories		$P_{acc} = P_{heat} + P_{cool} + P_{el}$	5,27
$\boldsymbol{P_{heat}}$ [W] hot air conditioning power demand; $\boldsymbol{P_{cold}}$ [W] cold air conditioning power demand; $\boldsymbol{P_{elec}}$ [W] electronic power demand from the engine.			
Computed Parameter	**N°**	**Equation**	**Source**
H- Differential Efficiencies			
Gasoline Engine		$\eta_{d,GV} = (1 - r_c^{1-\gamma} - \phi_{FA} - \mathrm{q} + m)$	
Electric Engine		$\eta_{d,BEV} = (1 - \delta)$	
Drivetrain		$\eta_{i,dr} = c$	
Battery		$\eta_{d,bat} = \eta_{charging}$	
Regen.		$\eta_{d,regen} = 1 - \frac{(2B - B_{lim})^2}{4B^2}$	
I- Power Integration			
Energy Loss per distance		$E_{loss} = \frac{1}{d}\int P_{loss}(t)dt$	
$\boldsymbol{P_{loss}}$ [W] sum of all the losses previously presented; **d** [m] distance traveled.			
J- Conversion from energy demand to energy consumption			
Conversion		$EC_{loss} = \frac{1}{\Lambda}E_{loss} \quad \begin{cases}\Lambda_{GV} = 10LHV_g \\ \Lambda_{BEV} = 36\end{cases}$	1,11
$\boldsymbol{\Lambda}$ conversion factor; $\boldsymbol{LHV_g}$ [J/kg] Lower Heating Value of the gasoline.			

1.2 - Equations for the energy consumption of the vehicle

Table S2: Raw equations used in the methodology to parametrize ***energy consumption*** *of automobile. The colors identify the contributors: the car body (in blue), the powertrain (in orange) and the dynamic variables (in gray) which are functions of the driver and the path.*

Driver	Result for GV	Results for BEV
A- External Forces		
Rolling	$EC_{rolling,GV} = \frac{r_0 M g J_{1,GV}}{\Lambda_{GV}\eta_{d,GV}\eta_{d,dr}}$	$EC_{rolling,BEV} = \frac{r_0 M g}{\Lambda_{BEV}\eta_{d,BEV}\eta_{d,dr}\eta_{d,bat}}$
Aerodynamic drag	$EC_{aero,GV} = \frac{0.5\,\rho C_D A \mathcal{J}_{3,GV}}{\Lambda_{GV}\eta_{d,GV}\eta_{d,dr}}$	$EC_{aero,BEV} = \frac{0.5\,\rho C_D A \mathcal{J}_{3,BEV}}{\Lambda_{BEV}\eta_{d,BEV}\eta_{d,dr}\eta_{d,bat}}$
Inertia & Rotating Inertia	$EC_{inertia,GV} = \frac{(M + \frac{4I_w}{r_w^2})K_1}{\Lambda_{GV}\eta_{d,GV}\eta_{d,dr}}$	$EC_{inertia,BEV} = \frac{(M + \frac{4I_w}{r_w^2})(1 - \eta_{regen})K_1}{\Lambda_{BEV}\eta_{d,BEV}\eta_{d,dr}\eta_{d,bat}}$
Grade	$EC_{grade,GV} = \frac{r_0 M g \mathcal{H}}{\Lambda_{GV}\eta_{d,GV}\eta_{d,dr}}$	$EC_{grade,BEV} = \frac{r_0 M g \mathcal{H}}{\Lambda_{BEV}\eta_{d,BEV}\eta_{d,dr}\eta_{d,bat}}$

Additional drag due to wind	$EC_{wind,GV} = \frac{0.5\,\rho C_D A W}{\Lambda_{GV}\eta_{d,GV}\eta_{d,dr}}$	$EC_{wind,BEV} = \frac{0.5\,\rho C_D A W}{\Lambda_{BEV}\eta_{d,BEV}\eta_{d,dr}\eta_{d,bat}}$
r_0 [-] rolling factor; **M** [kg] vehicle weight; ρ [-] air density; C_d [-] drag coefficient; **A** [m^2] vehicle frontal area; I_w [] polar moment of the inertia of the wheels; r_w [m] effective radius of the wheels; $J_1\ [-], J_3\ [m^2/s^2], K_1 [m/s^2], \mathcal{H}\ [-], W$ [m^2/s^2] dynamic variable integrals of the speed, the speed cube, the inertia, the slope and the wind; Λ conversion factor; $\eta_{d,GV}\ [-], \eta_{d,BEV}\ [-], \eta_{d,dr}\ [-],\ \eta_{d,bat}$ [-] differential efficiencies of resp. the gasoline engine, the electric engine, the drivetrain and the battery. Subletters GV refer to gasoline vehicles and BEV to electric vehicles.		
A- Gasoline Engines Losses (only for GV)		
Frictions	$EC_{fr,GV} = \frac{fmep_0 D(\mathcal{L}_{1,GV} + N_{idle}t_{idle})}{4\pi\Lambda_{GV}\eta_{d,GV}}$	
Thermal	$EC_{thermal,GV} = \frac{Q_0 D(\mathcal{J}_{0,GV} + t_{idle})}{4\pi\Lambda_{GV}\eta_{d,GV}}$	
Pumping	$EC_{pump,GV} = \frac{p_0 D(\mathcal{L}_{3,GV} + N_{idle}^3 t_{idle})}{4\pi\Lambda_{GV}\eta_{d,GV}}$	
Cold Start	$EC_{cs,GV} = \frac{c_s P_e}{d\Lambda_{GV}\eta_{d,GV}\eta_{d,dr}}$	
$fmep_0$ [kPa] friction mean pressure at no load; **D** [L] engine displacement; Q_0 [kPa/s] insulation losses at no load; p_0 [kPa.s2] pumping mean effect at no load; c_s [J/W/m] cold start constant; N_{idle} [rad/s] the engine speed during idling; P_e [W] maximum power of the engine; $\mathcal{L}_1\ [m^{-1}], \mathcal{L}_3\ [s^{-2}], J_0[s.m^{-1}],\ t_{idle}[s.m^{-1}]$ dynamic variable integrals of the engine speed, the engine speed cube, the time, and the idling time; Λ conversion factor; $\eta_{d,GV}\ [-],\ \eta_{d,dr}\ [-]$ differential efficiencies of resp. the gasoline engine and the drivetrain; **d** [m] distance traveled.		
B- Electric Engines Losses (only for BEV)		
Conductive	$EC_{copper,BEV} = \frac{\varepsilon\,\mathcal{T}_2}{\Lambda_{BEV}\eta_{d,BE}\eta_{d,bat}}$	
Converter	$EC_{converter,BEV} = \frac{\beta\,J_{0,BEV}}{\Lambda_{BEV}\eta_{d,BE}\eta_{d,bat}}$	
Friction	$EC_{fr,BEV} = \frac{\alpha\,\mathcal{L}_{1,BEV}}{\Lambda_{BEV}\eta_{d,BE}\eta_{d,bat}}$	
$\alpha\,[J], \beta[W], \delta[-], \varepsilon[s.kg^{-1}]$ electric engine characteristic constant; $\mathcal{L}_1\ [m^{-1}]$,$J_0[s.m^{-1}]$, $\mathcal{T}_2\ [N^2.s.m^{-1}]$ dynamic variable integrals of the engine speed, the time, and the square torque; $\eta_{d,BEV}\ [-], \eta_{d,bat}\ [-]$ differential efficiencies of resp. the electric engine and the battery. Λ conversion factor.		
C- Drivetrain Losses		
Frictions	$EC_{trans,GV} = \frac{a_{tr}P_e\mathcal{L}_{1,GV}}{\Lambda_{GV}\eta_{d,GV}\eta_{d,dr}}$	$EC_{trans,BEV} = \frac{a_{tr}P_e\mathcal{L}_{1,BEV}}{\Lambda_{BEV}\eta_{d,BEV}\eta_{d,dr}\eta_{d,bat}}$
Synchronization	$EC_{synchro,GV} = \frac{r_{urban}S}{\Lambda_{GV}\eta_{d,GV}}$	Not concerned
P_e [W] maximum power of the engine; a_{tr} [s] drivetrain characteristic constant; **S** [J/m] synchronization loss constant; $\mathcal{L}_1\ [m^{-1}]$ dynamic variable integrals of the engine speed; r_{urban} [-] share of the distance traveled in urban area; $\eta_{d,GV}\ [-], \eta_{d,BEV}\ [-], \eta_{d,dr}\ [-],\ \eta_{d,bat}$ [-] differential efficiencies of resp. the gasoline engine, the electric engine, the drivetrain and the battery.		
Battery Losses (only for BEV)		
Driving	$EC_{discharg,,BEV} = \frac{R\mathcal{P}_2}{U^2\Lambda_{BEV}\eta_{d,bat}}$	
R [ohm] internal resistance of the battery; **U** [V] battery voltage; $\mathcal{T}_2\ [W^2.s.m^{-1}]$ dynamic variable integrals of the square power; Λ conversion factor; $\eta_{d,bat}\ [-]$ differential efficiencies of the battery.		
Accessories Losses		
Accessories	$EC_{acc,GV} = \frac{P_{acc}\,(J_{0,GV} + t_{idle})}{\Lambda_{GV}\eta_{d,GV}}$	$EC_{acc,BEV} = \frac{P_{acc}\,(J_{0,BEV} + t_{idle})}{\Lambda_{BEV}\eta_{d,BEV}\eta_{d,bat}}$
$P_{acc} = (P_{heat} + P_{cold} + P_{elec})$ [W] total power of accessories; $J_0[s.m^{-1}], t_{idle}[s.m^{-1}]$ dynamic variable integrals of the time and idling time. $\eta_{d,GV}\ [-],\ \eta_{d,BEV}\ [-], \eta_{d,bat}\ [-]$ differential efficiencies of resp. the electric engine and the battery; Λ conversion factor.		

1.3 – Dynamic variables integrals parametrization

Table S3: Raw equations used in the methodology to parametrize ***the dynamic variables integrals****. The colors identify the contributors: the car body (in blue), the powertrain (in orange), the driver (in green) and the path (in red).*

Variable	GV	BEV
av	$K_1 = \mu_v^2 K_{1,p}$	
av^2	$K_2 = \mu_v^3 K_{2,p}$	
v	$J_{1,GV} = \left(1 - \frac{\mu_v^2 K_{1,p}}{B}\right)$	$J_{1,el} = 1$
v^3	$J_{3,GV} = \mu_v^2 J_{3,p}\left(1 - \frac{\mu_v^2 K_{1,p}}{B} - \frac{M\mu_v^3 K_{2,p}}{\mu_a P_e}(1 - r_{acc}^2)\right)$	$J_{3,BEV} = \mu_v^2 J_{3,p}\left(1 - \left(\frac{\mu_v^2 K_{1,p}}{B} + \frac{M\mu_v^3 K_{2,p}}{\mu_a P_e}\right)(1 - r_{acc}^2)\right)$
1	$J_{0,GV} = \frac{1}{\mu_v} J_{0,p}\left(1 - \frac{\mu_v^2 K_{1,p}}{B} - \frac{M\mu_v^3 K_{2,p}}{\mu_a P_e}(1 - r_{acc}^2)\right)$	$J_{0,BEV} = \frac{1}{\mu_v} J_{0,p}\left(1 - \left(\frac{\mu_v^2 K_{1,p}}{B} + \frac{M\mu_v^3 K_{2,p}}{\mu_a P_e}\right)(1 - r_{acc}^2)\right)$
N	$\mathcal{L}_{1,GV} = \left(r_{urban}\frac{\mu_N N_e}{\mu_v} J_{0,p} + r_{rural}\sigma_r\right)\left(1 - \frac{\mu_v^2 K_{1,p}}{B} - \frac{M\mu_v^3 K_{2,p}}{\mu_a P_e}\right) + \frac{N_a M \mu_v^2 K_{1,p}}{\mu_a P_e}$	$\mathcal{L}_{1,elec} = \sigma_{elec}$
N^3	$\mathcal{L}_{3,GV} = \left(r_{urban}\frac{(\mu_N N_e)^3}{\mu_v} J_{0,p} + r_{rural}\sigma_r \mu_v^2 J_{3,p}\right)\left(1 - \frac{\mu_v^2 K_{1,p}}{B} - \frac{M\mu_v^3 K_{2,p}}{\mu_a P_e}\right) + \frac{N_a^3 M \mu_v^2 K_{1,p}}{\mu_a P_e}$	Not needed
T^2	Not needed	$\mathcal{T}_2 = \frac{\mu_a T_{max}^2 M \mu_v^2 K_{1,p}}{\mu_a P_e}$
P_{in}^2	Not needed	$\mathcal{P}_2 = (\mu_a P_e M \mu_v^2 K_{1,p}) + E_{cruise}^2 / J_{0,BEV}$
$v.si$	$\mathcal{H} = h$	
$v.v_v^2$	$W = w^2\left(1 - \frac{\mu_v^2 K_{1,p}}{B}\right)$	$W = w^2$

<u>Parameters for the driver</u>:
μ_v $[-]$ Driver speed compliance ratio; B [m/s²] mean deceleration by the driver during braking; μ_a $[-]$ Driver acceleration aggressiveness; μ_N $[-]$ Driver engine speed aggressiveness; N_a [rad/s] engine speed during acceleration.

<u>Parameters for the path</u>:
$\mathcal{K}_{1,p}$ $[m/s^2]$, $\mathcal{K}_{2,p}$ $[m^2/s^3]$, $\mathcal{J}_{0,p}$ $[s/m]$, $\mathcal{J}_{3,p}$ $[m^2/s^2]$, h $[-]$ and w $[m/s]$ are the dynamic variables integrals evaluated with the target functions which only depends on the path.
r_{urban} $[-]$ and r_{rural} $[-]$ are resp. the share of the journey traveled in urban area and rural area.
r_{acc} $[-]$ the ratio of average speed during acceleration to the final cruising speed.

<u>Other parameters</u>:
M [kg] the vehicle weight; σ_{elec} [-] the BEV drive ratio; σ_r [-] the GV drive ratio in rural areas; N_e [rad/s] the GV default engine speed in urban area; P_e [W] maximum power of the engine; T_{max} [N] maximum torque of the engine;

1.4 – Example of PIEC equations

*Table S4: Raw equations to **some PIEC**.*

Parameter	Result for GV	Unit
B- External Forces		
Mass (M)	$MIEC = \frac{100}{36} \cdot \frac{1}{\eta_{d,e}\eta_{d,dr}\eta_{d,bat}} (r_0 g J_1 + (1 - \eta_{regen})K_1 + g\mathcal{H})$	kWh/100km/100kg
Drag (Cd)	$C_d IEC = \frac{1}{360} \cdot \frac{0.5\rho A(J_3 + w^2 J_1)}{\eta_{d,e}\eta_{d,dr}\eta_{d,bat}}$	kWh/100km/unit-
Rolling factor (r0)	$r_0 IEC = \frac{1}{36000} \cdot \frac{M g J_1}{\eta_{d,e}\eta_{d,dr}\eta_{d,bat}}$	kWh/100km/0.001-
Engine Displacement (GV) (D)	$DIEC = \frac{1}{36} \cdot \frac{\boldsymbol{fmep_0}(\boldsymbol{\mathcal{L}_{1,GV}} + \boldsymbol{N_{idle} t_{idle}}) + \boldsymbol{Q_0 D}\left(\boldsymbol{J_{0,GV}} + \boldsymbol{t_{idle}}\right) + \boldsymbol{p_0 D}(\boldsymbol{\mathcal{L}_{3,GV}} + \boldsymbol{N_{idle}^3 t_{idle}})}{\eta_{d,e}\eta_{d,dr}\eta_{d,bat}}$	kWh/100km/L
Gear ratio (BEV) (D)	$\sigma IEC = \frac{1}{36} \cdot \frac{\alpha + a_{tr} P_e}{\eta_{d,e}\eta_{d,dr}\eta_{d,bat}}$	kWh/100km/unit-

2- Energy Consumption from Power Demand

In this section, a detailed analysis of all losses from the battery to the external forces are presented (figure S1). For each loss:
(1) an equation characterizing the power loss is determined.
(2) if the power loss is proportional to the power demand, the differential efficiency associated to this loss is computed.
(3) otherwise, the power losses are integrated over time. Three steps are required: (a) propagation of the differential efficiencies, (b) introduction of the cycle variables, and (c) conversion of the energy demand into energy consumption. Further explanations for these three steps are given in the following section.

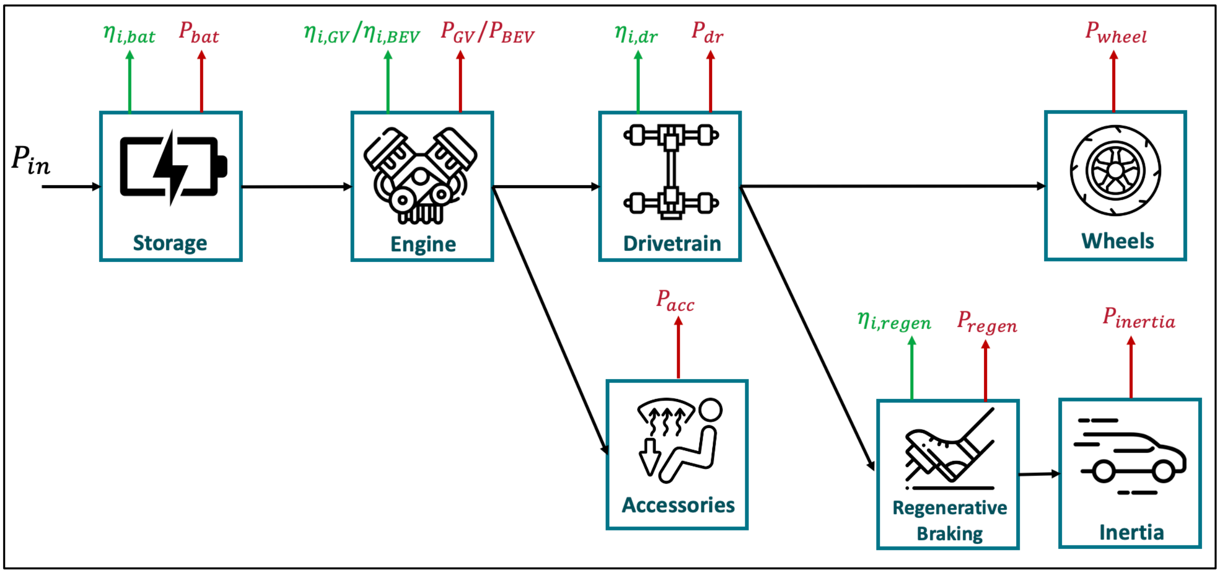

Figure S1: Graphical representation of the energy conversion steps from tank to wheel. For each element (names in red), the losses independent to the power demand (red arrows) and the differential efficiencies (green arrows) are calculated.

2.1- Presentation of the steps for converting power losses into energy consumption

2.1.1) Propagation of differential efficiencies

As represented in the Figure S2, a given element (e) of the powertrain is supplied by a power $P_{in,e}$ and furnished the power $P_{out,e}$. The difference between the power in and out corresponds to the losses occurring during the energy conversion in the element. In this paper, the term *efficiency* is limited to *differential efficiency* ($\eta_{i,e}$) , which describes the losses that are proportional to the power supplied, as defined by Rohde-Brandenburger[28] in equation S1:

$\sum_{loss} P_{loss} = (1 - \eta_{i,e})P_{in,e}$ (Equation S1)

All other losses that are independent of power demand are treated as separate contributions to vehicle consumption ($\sum_{contrib} P_{contrib}$).

Consequently, the equation S2 links the power supplied to the element ($P_{in,e}$) and the power out of the element ($P_{out,e}$):

$$P_{in,e} = P_{out,e} + \sum_{loss} P_{loss} = P_{out,e} + (1 - \eta_{i,e})P_{in,e} + \sum_{contrib} P_{contrib}$$

$\Leftrightarrow P_{in,e} = \frac{1}{\eta_{i,e}} P_{out,e} + \frac{1}{\eta_{i,e}} \sum_{contrib} P_{contrib}$ (Equation S2)

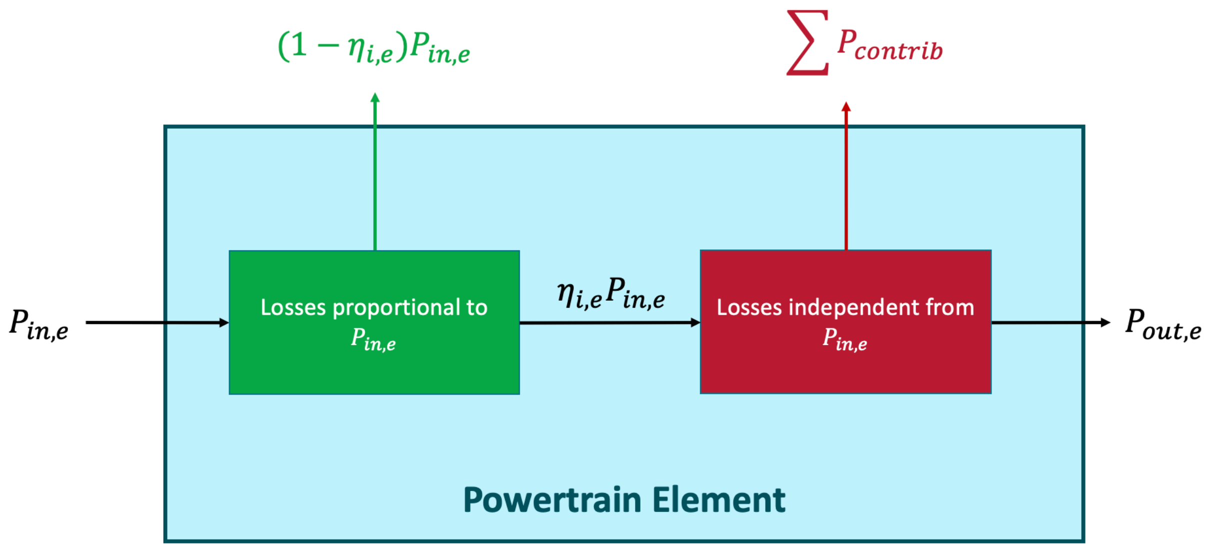

Figure S2: Graphical representation of the losses in a powertrain element. This power supplied ($P_{in,e}$) is equal to the sum of the power required out of the system ($P_{out,e}$) and the power lost. The losses are separated in two categories: the losses proportional to the power supplied and the losses that are independent of this power supplied.

As seen in the figure S1, the powertrain elements are organized following the energy conversion and transmission from tank to wheels. The power out of an element corresponds to the power supplied to the following element. Therefore, the differential efficiencies of an element applied to the losses of all subsequent elements of the powertrain. For example, the power loss to overcome the external forces are divided by the differential efficiencies of all powertrain elements.

2.1.2) Dynamic variable integrals

To obtain the energy consumption associated to a power loss, this power loss should be integrated over time as shown in Equation S3:

$E_{in} = \frac{1}{d} \int P_{in}(t)dt$ (Equation S3)

Therefore, all dynamic variables introduced in the power loss equations (e.g. speed, engine speed, torque) should be integrated over time. The following notation are used to parametrize these integrals:

$K_1 = \frac{1}{d}\int avdt;$
$K_2 = \frac{1}{d}\int av^2dt;$
$J_0 = \frac{1}{d}\int dt;$
$J_1 = \frac{1}{d}\int vdt;$
$J_3 = \frac{1}{d}\int v^3dt;$
$\mathcal{L}_1 = \frac{1}{d}\int N\,dt;$
$\mathcal{L}_3 = \frac{1}{d}\int N^3\,dt;$
$\mathcal{T}_2 = \frac{1}{d}\int T^2\,dt;$
$\mathcal{P}_2 = \frac{1}{d}\int P^2\,dt;$
$\mathcal{H} = \frac{1}{d}\int v sin\theta\,dt;$
$W = \frac{1}{d}\int vv_{wind}^2\,dt$

The section 3 of this document will present the original approach developed to calculate these parameters as a function of the path and the driver behavior.

2.1.3) Conversion of energy demand in vehicle's energy consumption

The Energy demand E_{in} obtained in Equation SI-28 is given in [J/m] and should be converted in $[l/100km]$ for GV and in $[kWh/100km]$ for BEV. For GV, the energy demand is converted into gasoline volume using the lower heating value LHV_g of the gasoline, which is given in $[MJ/L]$. To obtain $[l/100km]$, the energy demand is multiplied by a factor 10^5 and the LHV by a factor 10^6. Finally, we obtain the following equation:

$$EC_{GV}\ [l/100km] = \frac{10^5 E_{in}}{10^6 LHV_g} = \frac{1}{10LHV_g}E_{in}$$

Regarding BEV, energy demand is multiplied by a factor 10^5 to convert it per 100km and converted in kWh with the ratio $1kWh = 3.6\ 10^6$. Finally, we obtain the following equation:

$$EC_{BEV}\ [kWh/100km] = \frac{10^5}{3.6\ 10^6}E_{in} = \frac{1}{36}E_{in}$$

The conversion is generalized by introducing a conversion factor Λ that depends on the powertrain (Equation S4):

$$EC = \frac{1}{\Lambda}E_{in} \quad \begin{cases} \Lambda_{GV} = 10LHV_g \\ \Lambda_{BEV} = 36 \end{cases} \quad \text{(Equation S4)}$$

2.2- Equations the energy consumption from battery to external forces

2.2.1) Battery Losses

Charging Process

Charging losses can be modeled by a constant loss $P_{charging}$ $[W]$ due to AC/DC conversion and internal resistances [22,23]. As P_{out} [W] the power of the supplied to charge the battery is also constant, the energy consumed by the charging loss is proportional to the energy demand as shown by the following calculations:

$P_{in} = (P_{charging} + P_{out}) \Leftrightarrow P_{charging} = (1 - \eta_{charg})P_{in}$ (Equation S5)

With $\eta_{charg} = \frac{P_{out}}{P_{charging}+P_{out}}$

Discharging Process

For driving losses in the battery, the power that travels in the battery is not constant anymore. The voltage *U [V]* of the battery is considered constant while the intensity *I [A]* varies as a function of the power demand. As shown by the literature[21,22], the power furnished or stored by the battery and the intensity are proportional based on electric properties:

$$P = UI$$

This relationship leads to the final equation of the battery losses for discharging and for regenerative charging:

$P_{discharging} = R(\frac{P_{in,bat}}{U})^2$ (Equation S6)

R [ohm] is the internal resistance of the battery, *U [V]* the voltage, $P_{in,bat}[W]$ the power demand of the battery.

Differential efficiency of the battery and energy consumption of other losses

By summing the terms proportional to P_{in}, the equation S7 is obtained for differential efficiency of the battery:

$\eta_{bat} = \eta_{charging}$ (Equation S7)

Other losses which are not proportional to P_{in}, they lead to energy consumption independent to other losses. After integration, the expression S8 is obtained.

$\boldsymbol{EC_{discharg,BEV}} = \frac{\boldsymbol{R\mathcal{P}_2}}{\mathbf{U^2}\boldsymbol{\Lambda_{BEV}\eta_{i,bat}}}$ (Equation S8)

2.2.2) Gasoline Engine Losses

Thermodynamic and injection Losses

The engine in this model operates on the Otto cycle, which directly determines its thermodynamic efficiency. The thermodynamic losses are expressed by the equation S9[4,9].

$P_{thermo} = \frac{1}{r_c{}^{\gamma-1}}P_{in}$ (Equation S9)

where r_c represents the compression ratio, and γ is the specific heat ratio of the working fluid, typically around 1.4 for air and $P_{in}[W]$ the power demand.

Moreover, injection losses are also considered. It refers to the reduction in efficiency due to deviations from the ideal fuel-air cycle. The loss is characterized by the equation S10[1,4]

$P_{inj} = \phi_{FA} P_{in}$ (Equation S10)

With ϕ_{FA} $[-]$ representing the fuel-air ratio relative to stoichiometric.

P_{thermo} and P_{inj} are calculated in [W].

Friction and pumping Losses

Friction losses represent the energy dissipated as heat due to friction between the moving parts within an engine. This phenomenon occurs because various engine components, such as the pistons, crankshaft, camshaft, and valves, must overcome internal resistance as they move and interact. In the literature, these friction losses are often modeled as being proportional to engine displacement *D [L]* and engine speed *N [rad/s]* [4,10,11]. For pumping loss, several different expressions have been found in the literature. Sandoval et al.[14] demonstrated that a significant portion of these losses can be attributed to "pumping," with valve pumping losses and intake manifold losses being the most significant contributors. Yagi et al.[13] showed that part of the pumping was proportional to N^3 , which aligns with Sandoval's findings for valve pumping losses. Ross[4] proposed a model for manifold loss: at no load, manifold losses are proportional to engine speed and displacement (like mechanical losses), but manifold is also dependent on the torque as it decreases proportionally with power demand. This description is consistent with Sandoval's model. All other terms introduced by Sandoval are neglected. In our model, the frictions and the manifold losses have been compiled in P_{fr} (Eq. S11) and the valve pumping loss is expressed in P_{pump} (Eq. S12).

$P_{fr} = \frac{fmep_0 DN}{4\pi} - mP_{in}$ (Equation S11)

$P_{pump} = \frac{p_0}{4\pi} DN^3$ (Equation S12)

$fmep_0$ $[kPa]$ represents the friction loss at no load due to mechanical friction and the manifold loss.

mP_{in} indicates the reduction in manifold loss as the throttle opens.

p_0 $[kPa.s2]$ represents the pumping loss at no load due to valve pumping loss.

N $[rad/s]$ is the engine speed.

D $[L]$ represents the engine displacement.

P_{fr} and P_{pump} are calculated in [W].

NB: The 4π comes from the conversion from Ross equation where N is given in rotation per second to SI unit for N in rad/s.

Thermal Losses

Thermal losses can be divided into two categories: losses due to the partial thermal energy of the combustion that is lost (incomplete combustion) and the thermal energy consumed to maintain the engine at its operating temperature[4,12]. Based on the model from Muranaka et al.[12], it has been determined that incomplete combustion led to a loss proportional to the power demand while the heat loss through the wall of the engine can be modeled with a constant loss proportional to the size of the cylinders characterized by the displacement:

$P_{thermal} = (Q_0 D + qP_{in})$ (Equation S13)

With Q_0 $[kPa/s]$ and q $[-]$ constant depending on the engine insulation and performances.

Cold Start

Cold start conditions lead to additional losses at the beginning of a trip because the engine is not yet at its optimal operating temperature. A cold engine experiences more losses than a hot engine due to increased internal friction and inefficient fuel combustion. As no simplified equations have been found, the cold start has been modeled based on average values from the EPA engines[15]. The average energy lost per trip due to cold start is modeled with the equation S14:

$E_{cs} = c_s P_e$ (Equation S14)

With c_s $[s]$ a constant calculated based on EPA testing.

Idling

During idling, all losses (thermodynamics, friction, pumping and thermal losses) continue to consume energy. The engine operates at no load, with an engine speed at idle N_{idle} that depends on the engine. The energy consumed due to idling has been directly included in the contribution of the losses. Note that for engine equipped with start-and-stop system, idling is neglected. The losses due to idling become null.

Differential efficiency of the gasoline engine and energy consumption of other losses

By summing the terms proportional to P_{in}, the equation S15 is obtained for differential efficiency of the gasoline engine:

$\eta_{i,GV} = (1 - r_c^{1-\gamma} - \phi_{FA} - \mathrm{q} + m)$ (Equation S15)

Other losses which are not proportional to P_{in}, they lead to energy consumption independent to other losses. After integration, the expressions S16 to S19 are obtained.

$EC_{fr,GV} = \frac{fmep_0 D(\mathcal{L}_{1,GV} + N_{idle} t_{idle})}{4\pi \Lambda_{GV} \eta_{i,GV}}$ (Equation S16)

$EC_{thermal,GV} = \frac{Q_0 D(J_{0,GV} + t_{idle})}{4\pi \Lambda_{GV} \eta_{i,GV}}$ (Equation S17)

$EC_{pump,GV} = \frac{p_0 D(\mathcal{L}_{3,GV} + N_{idle}^3 t_{idle})}{4\pi \Lambda_{GV} \eta_{i,GV}}$ (Equation S18)

$$EC_{cs,GV} = \frac{c_s P_e}{d\Lambda_{GV}\eta_{i,GV}\eta_{i,dr}}$$ (Equation S19)

2.2.3) Electric Engine Losses

Mahmoudi[16] and Roshandel[17] demonstrates that four main losses occurred in electric engines: copper loss, core loss, converter losses and mechanical losses. From the efficiency maps they built and from their different reviews, they concluded that copper loss can be considered in most technologies as proportional to the square of the torque T^2. Core loss are proportional to power demand. We can suppose that mechanical losses are proportional to engine speed as for gasoline engine case, and that converter losses are constant. Finally, we obtain the equation proposed in the paper for the power loss of electric engine (Eq. S20)

$$P_{losses} = \delta P_{in} + \varepsilon T^2 + \alpha N + \beta$$ (Equation S20)

With P_{in} [W] the power demand of the engine; N [rad/s] the engine speed; T [N] the engine torque; $\alpha\ [J], \beta[W], \delta[-], \varepsilon[s.kg^{-1}]$ electric engine characteristic constants.

<u>Differential efficiency of the electric engine and energy consumption of other losses</u>

By summing the terms proportional to P_{in}, the equation S21 is obtained for differential efficiency of the electric engine.

$$\eta_{i,BEV} = 1 - \delta$$ (Equation S21)

Other losses which are not proportional to P_{in}, they lead to energy consumption independent to other losses. After integration, the expressions S22 to S24 are obtained.

$$EC_{copper,BEV} = \frac{\varepsilon\, \mathcal{T}_2}{\Lambda_{BEV}\eta_{i,BE}\eta_{i,bat}}$$ (Equation S22)

$$EC_{converter,BEV} = \frac{\beta\, J_{0,BEV}}{\Lambda_{BEV}\eta_{i,BE}\eta_{i,bat}}$$ (Equation S23)

$$EC_{fr,BEV} = \frac{\alpha\, \mathcal{L}_{1,BEV}}{\Lambda_{BEV}\eta_{i,BEV}\eta_{i,bat}}$$ (Equation S24)

2.2.4) Accessories

Accessories demand can be decomposed in three parts[5,27] : the power from electronic of the car, the air conditioning for cooling the vehicle in summer and the heating of the vehicle in winter. The power demand from the accessories of the vehicle can thus be written with equation S25.

$P_{acc} = P_{heat} + P_{cool} + P_{el}$ (Equation S25)

With P_{heat} [W], P_{cool} [W] , P_{el} [W] the power of resp. the heat demand, the cooling demand, and the electronic demand.

Energy consumption of accessories

By considering that the power demand from the accessories in constant over time, the equation S26 and S27 are obtained to compute the energy consumption of accessories.

$\boldsymbol{EC_{acc,GV}} = \frac{\boldsymbol{P_{acc}}\,(\boldsymbol{J_{0,GV}})}{\boldsymbol{\Lambda_{GV}\eta_{e,GV}}}$ for the GV. (Equation S26)

$\boldsymbol{EC_{acc,BEV}} = \frac{\boldsymbol{P_{acc}}\,(\boldsymbol{J_{0,BEV}})}{\boldsymbol{\Lambda_{BEV}\eta_{i,BEV}\eta_{i,bat}}}$ for the BEV. (Equation S27)

2.2.5) Drivetrain

Literature review showed that the drivetrain losses can be classified in three categories: the friction losses in the gearbox, the friction losses in the driveline and the synchronization losses in the gearbox [18–20].

Synchronization in the gearbox

Synchronization losses occur in the gearbox only during launches of the vehicle and gearshifts. Thus this loss is specific to thermal vehicles equipped with gearboxes. Based on the works of Habermehl with different driving cycles that synchronization on highway is negligeable. We illustrate in the excel file (Supplementary Information SI-2) that the synchronization energy demand is proportional to the distance traveled in urban area, leading to equation S28.

$E_{synchro,u} = S.\,d_{urban}$ (Equation S28)

With S [J/m] the synchronization loss constant and d_{urban} [m] the distance traveled in urban area.

Frictions in the gearbox and driveline

Friction losses are due to friction between the parts of the transmission, occurring in the gearbox and along the axles that composes the drivetrain. It has been demonstrated that a part of mechanical frictions is torque dependent while another part is torque independent, solely proportional to the engine speed and the size of the engine[18,19]. For these reasons, the transmission has been modeled with the following expression S29 which is valid for both gasoline engines and electric engines.

$P_{trans} = \ (a_{tr}P_eN + cP_{in})$ (Equation S29)

With P_{out} [W] the power supplied to the drivetrain; N [rad/s] the engine speed; P_e [W] the maximum power of the engine and a_{tr} [s], c [-] drivetrain characteristic constants.

Differential efficiency of the drivetrain and other independent losses

By summing the terms proportional to P_{in}, the equation S30 is obtained for differential efficiency of the drivetrain:
$\eta_{dr} = c$ (Equation S30)

Other losses which are not proportional to P_{in}, they lead to energy consumption independent to other losses. After integration, the expressions S31 and S32 are obtained for GV.

$$\boldsymbol{EC_{trans,GV}} = \frac{a_{tr} P_e \mathcal{L}_{1,GV}}{\Lambda_{GV} \eta_{i,GV} \eta_{i,dr}} \text{ (Equation S31)}$$

$$\boldsymbol{EC_{synchro,GV}} = \frac{r_{urban} S}{\Lambda_{GV} \eta_{i,GV}} \text{ (Equation S32)}$$

And Equation S33 is obtained for BEV.

$$\boldsymbol{EC_{trans,BEV}} = \frac{a_{tr} P_e \mathcal{L}_{1,BEV}}{\Lambda_{BEV} \eta_{i,BEV} \eta_{i,dr} \eta_{i,bat}} \text{ (Equation S33)}$$

2.2.6) Regenerative Losses

Regenerative braking is a system in automobiles that captures the energy typically lost during braking by converting it into electrical energy. This recovered energy is then stored in the vehicle's battery and can be used to power the car. This section aims to estimate the proportion of inertia that can be recovered.

The serial strategy as depicted by Qiu et al.[29] is modeled in this paper (see figure S2). Regenerative braking is used during braking until it reaches a limit of braking force. This limit is reached when maximum braking power that the engine or the battery can produce[26] or for safety measures[25]. In his paper, Ruan[25] demonstrates that for safety optimization, braking deceleration recovered by regenerative braking should not exceed 0.13g, i.e around B_{lim}=1.3 m/s-2. For deceleration above the limit, the supplementary deceleration is provided by mechanical braking, which cannot be recovered by the engine.

The analysis of the driving cycles enables to estimate the mean braking deceleration provided by the driver B exerts on the vehicle. From the analysis, we also noticed that the maximum braking deceleration of the vehicle is around $2B$. We consider in the following a uniform distribution of decelerations between 0 and $2B$.

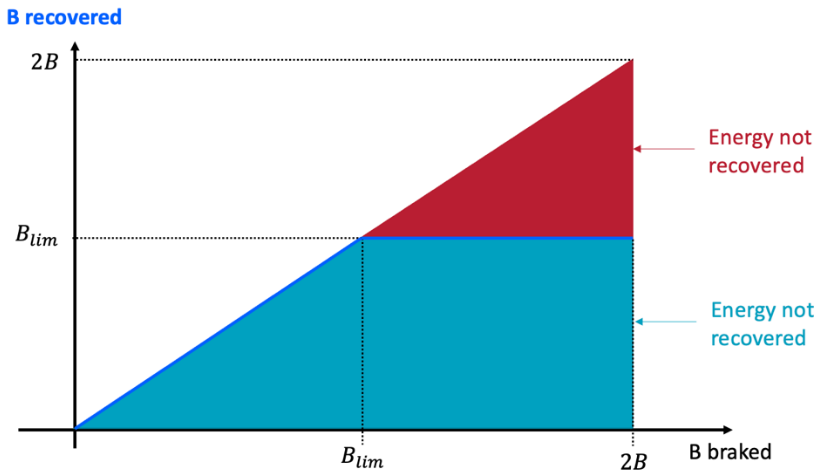

Figure S3: Graphical representation of the safety limit of regenerative braking. All kinetic energy is recovered when the braking deceleration is lower that this safety limit. For deceleration superior to the limit, mechanical braking is used to provide the additional deceleration, this energy cannot be recovered.

As seen in the figure S3, the share of the energy from braking that cannot be recovered is the proportion between red surface and blue surface. Considering a uniform distribution of the deceleration, we obtain that the proportion that is not recovered by the system is $\frac{(2B-B_{\text{lim}})^2}{4B^2}$.

It means that losses the amount of inertia that is lost due to the limit of braking deceleration recoverable is given by equation S34.

$P_{regen} = \frac{(2B-B_{\text{lim}})^2}{4B^2} P_{inertia}$ (Equation S34)

Which can be converted into an efficiency with equation S35.

$\eta_{regen} = 1 - \frac{(2B-B_{\text{lim}})^2}{4B^2}$ (Equation S35)

Where $P_{inertia}$ [W] is the power demand for inertia.
B [m/s^2] the mean deceleration during braking.
B_{lim} [m/s^2] the braking limit of regenerative braking deceleration.

Moreover, during braking, all other losses (external forces and powertrain losses) continue to consume energy. This energy consumed is lost and cannot be recovered. For this reason, all losses for BEV are integrated over the whole driving, while for gasoline engine, they are only integrated over acceleration and cruise when P>0 (during braking, no energy is consumed as the acceleration pedal is released).

2.2.7) External forces

For all external forces except wind

A consensus on the equation to characterize external forces that applies to a vehicle has been found in the literature and model reviewed for almost all the forces[1,3–5,8,11,30–39]. Based on this review, the equations S36 to S39 are used in our model.

For rolling, $P_{rolling} = r_0 Mgvcos\theta \approx r_0 Mgv$ (Equation S36)
For aerodynamic, $P_{aero} = 0.5\ \rho C_D A v^3$ (Equation S37)
For inertia and rotating inertia, $P_{inertia} = (\boldsymbol{M} + \frac{\boldsymbol{4I_w}}{\boldsymbol{r_w^2}})\frac{dv}{dt}v$ (Equation S38)
For grade, $P_{grade} = Mgvsin\theta$ (Equation S39)

With r_0 [-] the rolling factor; M [kg] the vehicle weight; v [m/s] the vehicle speed; ρ [-] the air density; C_d [-] the drag coefficient; A [m²] the vehicle frontal area; I_w [] the polar moment of the inertia of the wheels; r_w [m] the effective radius of the wheels; θ [rad] the road slope.

Wind effect

Tran et al., Swift, Miri et al. [6–8] showed that wind effect and aerodynamic drag are linked. The proper aerodynamic drag external force is given by the formula:

$$F_{realdrag} = \frac{\rho}{2} C_D A (v + v_{wind})^2$$

So that the power demand to overcome aerodynamic drag is:

$$P_{realdrag} = \frac{\rho}{2} C_D A v (v + v_{wind})^2$$

Where v_{wind} is the component of the wind speed vector in the direction of travel of the vehicle. This parameter can be positive or negative depending on its direction. This expression is valid under the hypothesis that $v + v_{wind} > 0$. The case $v + v_{wind} < 0$ is neglected as it concerns cases where wind speed is faster than the vehicle's speed, which is very unlikely.
To decouple the wind effect from the aerodynamic drag, the equation was developed to get on the one hand the aerodynamic drag (equation S37).
$P_{aero} = \frac{\rho}{2} C_D A v^3$ (Equation S37)
And on the other hand, the wind effect is given by equation S40.
$P_{wind} = \frac{\rho}{2} C_D A v v_{wind}^2$ (Equation S40)

The last term $\frac{\rho}{2} C_D A v (2 v v_{wind})$ is null when assuming that the wind direction is equally distributed in all directions.

Energy consumed to overcome external forces

The following table gather the equation obtained for characterizing the energy consumption of the external forces.

*Table S4: Raw equations used in the methodology to parametrize **energy consumption** of the external forces.*

GV	BEV
$EC_{rolling,GV} = \frac{r_0 M g J_{1,GV}}{\Lambda_{GV}\eta_{i,GV}\eta_{i,dr}}$	$EC_{rolling,BEV} = \frac{r_0 M g}{\Lambda_{BEV}\eta_{i,BEV}\eta_{i,dr}\eta_{i,bat}}$
$EC_{aero,GV} = \frac{0.5\,\rho C_D A \mathcal{J}_{3,GV}}{\Lambda_{GV}\eta_{i,GV}\eta_{i,dr}}$	$EC_{aero,BEV} = \frac{0.5\,\rho C_D A \mathcal{J}_{3,BEV}}{\Lambda_{BEV}\eta_{i,BEV}\eta_{i,dr}\eta_{i,bat}}$
$EC_{inertia,GV} = \frac{(M + \frac{4I_w}{r_w^2})K_1}{\Lambda_{GV}\eta_{i,GV}\eta_{i,dr}}$	$EC_{inertia,BEV} = \frac{(M + \frac{4I_w}{r_w^2})(1-\eta_{regen})K_1}{\Lambda_{BEV}\eta_{i,BEV}\eta_{i,dr}\eta_{i,bat}}$
$EC_{grade,GV} = \frac{r_0 M g \mathcal{H}}{\Lambda_{GV}\eta_{i,GV}\eta_{i,dr}}$	$EC_{grade,BEV} = \frac{r_0 M g h}{\Lambda_{BEV}\eta_{i,BEV}\eta_{i,dr}\eta_{i,bat}}$
$EC_{wind,GV} = \frac{0.5\,\rho C_D A w^2 J_{1,GV}}{\Lambda_{GV}\eta_{i,GV}\eta_{i,dr}}$	$EC_{wind,BEV} = \frac{0.5\,\rho C_D A w^2}{\Lambda_{BEV}\eta_{i,BEV}\eta_{i,dr}\eta_{i,bat}}$

3- Integration Model and calculation of the dynamic variable integrals

This section presents the original integration model that have been developed to calculate the dynamic variable integrals introduced in section 2.1 of this document. It is divided into three parts. First the assumptions presented in the main article are recapped. Second, few parameters useful for the integration model are computed. Third, the calculations of the dynamic variables integrals are performed.

3.1 - Assumptions and Parameters

(A1) *Speed - Cruise*: A constant cruise speed of the vehicle is assumed, neglecting minor speed fluctuations. These fluctuations are disregarded as they correspond to the natural deceleration of the vehicle due to friction and do not significantly affect inertia computation. The *real* cruise speed (v_{sect}) is defined in equation 1 with the ratio μ_v characterizing the driver's compliance with speed regulations (v_{path}).

$v_{sect} = \mu_v . v_{path}$ (Equation 1)

(A2) *Speed - Braking*: Braking corresponds to reducing the speed from v_{sect} to a given incident speed called v_{inc}. It is assumed that the driver steadily slows the vehicle using constant brake pressure. This results in a uniform deceleration, denoted as *B*, which is a driver-specific parameter reflecting their braking aggressiveness.

(A3) *Acceleration*: A continuous increase in speed is modeled by assuming constant power applied to the vehicle. This power, denoted as P_a, is defined in equation 2 where P_e is the maximum power available from the engine and μ_a represents the driver's utilization rate of this power, reflecting aggressiveness during acceleration phases.
$P_a = \mu_a P_e$ (Equation 2)

(A4) *Engine speed for BEV powertrain*: In BEV, which typically have a single gear, σ_{BEV} is constant. Neglecting tire slip, the engine speed of BEV (N_{BEV}) becomes proportional to the vehicle speed and can be expressed by equation 4.
$N_{BEV} = \sigma_{BEV} v_{sect}$ (Equation 4)

(A5) *Engine speed for ICEV powertrain*: For ICEV, $\mathrm{trans_g}(t)$ varies based on the engaged gear:

(A5a) In urban areas, gear shifts maintain a steady engine speed modeled by equation 5, where $\mathrm{N_e}$ represents the typical urban engine speed recommended for the engine, adjusted by the driver's aggressiveness factor μ_N.
$\mathrm{N_u} = \mu_\mathrm{N} \mathrm{N_e}$ (Equation 5)

(A5b) In rural areas, the highest gear is assumed remain engaged, making the engine speed proportional to vehicle speed and dependent solely on the gearbox ratio σ_f as shown by equation 6.
$\mathrm{N_r} = \sigma_f v_{sect}$ (Equation 6)

(A5c) During acceleration, engine speed $\mathrm{N_a}$ is considered constant. This parameter depends on the driver behavior.

(A6) *Squared Torque and Power*: According to the literature, torque is significant during acceleration phases but negligible during cruising [1,21]. Equation 8 simplifies the squared torque setting it equal to the squared torque at acceleration (T_a^2). Moreover, power demand differentiates between cruising and acceleration, following equation 9 to account for substantial power demands during acceleration (P_a^2) compared to cruising ($\tilde{P}_{cruise}$) which is averaged, obtaining a rectangular *target function* [1,21].
$T^2(t) = T_a^2 = \left(\frac{\mu_a P_{max}}{N_a}\right)^2$ (Equation 8)
$P^2(t) = P_a^2 + (\tilde{P}_{cruise})^2$ (Equation 9)

(A7) *Slope and Wind:* The model accounts for the average road slope (h) and wind speed (w) impacting the vehicle in each section.

3.2 - Computed Parameters

Here some useful computed parameters used in the following is calculated.

2.1) Inertia integration

$$K_1 = \frac{1}{d}\int_{P>0} a v dt = \frac{1}{d}\int_{P>0} \frac{dv}{dt} v dt = \frac{1}{2d}\int_{P>0} \frac{dv^2}{dt} dt$$

The path is modeled as a succession of cruise speed (v_{path}) and incidents (speed reduction to v_{inc}). K_1 is calculated by summing the variation of v^2 along the journey. When focusing on the path solely first, we obtain $K_{1,p}$ which is the dynamic variables integrals evaluated for the target function. The result is given in the equation S41.

$K_{1,p} = \frac{\sum_{inc}(v_{path}^2 - v_{inc}^2)}{2d}$ (Equation S41)

When considering driver behavior all speeds are increased by the driver aggressiveness factor (A1), the real function is integrated and K_1 is obtained in Equation S42.

$K_1 = \frac{\sum_{inc}(\mu_v^2 v_{path}^2 - \mu_v^2 v_{inc}^2)}{2d} = \mu_v^2 \, K_{1,p}$ (Equation S42)

In the same way, $K_{2,p}$ is calculated with equation S43.
$K_{2,p} = \frac{1}{d}\int_{P>0} av^2 dt = \frac{1}{3d}\int_{P>0} \frac{dv^3}{dt} dt = \frac{\sum_{inc}(v_{sect}^3 - v_{inc}^3)}{3d}$ (Equation S43)

And K_2in equation S44.
$K_2 = \mu_v^3 \, K_{2,p}$ (Equation S44)

2.2) *Braking Distance*

During braking, the deceleration B is supposed constant (A2). According to Newton's laws applied to the car for one incident:

$$a = -B$$
$$\Leftrightarrow v = v_{inc} - Bt$$
$$\Leftrightarrow x = x_0 + v_{inc}t - 0.5Bt^2$$

The duration of braking for one single incident can be calculated as:
$$v = v_{inc} - Bt \;\Leftrightarrow t_{bk,inc} = \frac{1}{B}(v - v_{inc})$$

Thus, $d_{bk,inc} = x - x_0 = v_{ini}t_{bk} - 0.5Bt_{bk}^2 = \frac{1}{2B}(v^2 - v_{inc}^2)$

By summing all incident, we obtain the equation S45 of the distance of braking during the path.

$d_{bk} = \frac{dK_1}{B}$ (Equation S45)

2.3) *Acceleration distance and duration*

During braking, the power P_a is supposed constant (A3). According to Newton's laws applied to the car for one incident is:

$$M\frac{dv}{dt}v = P_a \Leftrightarrow \frac{1}{2}v^2 = \frac{1}{2}v_{ini}^2 + \frac{P_a}{M}t$$

The duration of acceleration can be calculated with equation S46.

$t_a = \frac{(dK_1)M}{P_a}$ (Equation S46)

Then, $v = \sqrt{v_{ini}^2 - \frac{2P_a}{M}t} \Leftrightarrow x = \frac{M}{3P_a}\left(v^3 - v_{ini}^3\right)$

In other words, we obtain:

$d_{a,inc} = \frac{M}{3P_a}\left(v_{sect}^3 - v_{inc}^3\right)$

So that by summing, we obtain the distance of acceleration during the journey (eq. S47).

$d_a = \frac{M(dK_2)}{P_a}$ (Equation S47)

2.4) Average speed during acceleration and deceleration

As showed for deceleration, the square speed increases proportionally to the distance traveled. Thus, the average square speed during the deceleration is $\widetilde{v_f^2} - \widetilde{v_{inc}^2}$ with $\widetilde{v_f}$ is the average square speed of the vehicle after the end of the acceleration weighted by the intensity of the given incident and $\widetilde{v_{inc}}$ is the average square speed of incidents weighted by the intensity of the given incident. Estimation of these average speed is given by equation S48 and S49.

$\widetilde{v_{inc}^2} = v_{inc}^2 \frac{k_{inc}}{K}$ (Equation S48)

$\widetilde{v_f^2} = v_{sect}^2 \frac{k_{inc}}{K}$ (Equation S49)

The ratio r_{acc} is introduced as a measure of the speed reduction between the path target speed function and the real speed during acceleration and deceleration (Eq. S50).

$r_{acc} = \sqrt{\frac{\widetilde{v_f^2} - \widetilde{v_{inc}^2}}{\widetilde{v_f}^2}}$ (Equation S50)

2.5) Engine dynamic during acceleration

To model the impact of driver behavior during acceleration, it is assumed that the driver used a fraction μ_a of the maximum power available from the engine P_e (A3). We assume the following distribution of μ_a over N_a and T_a, knowing that N_a cannot be lower than N_{idle} (Eq. 51 and 52).

$T_a = \sqrt{\mu_a} T_{max}$ (Equation S51)

$N_a = \sqrt{\mu_a} (N_{max} - N_{idle}) + N_{idle}$ (Equation S52)

3.3 - Integration Variables Calculation

The calculation of dynamic variables integrals follows a two-step approach: first, the path *target functions* are integrated (Figure S4a), and then the results are adapted to the *real functions* (Figure S4b).

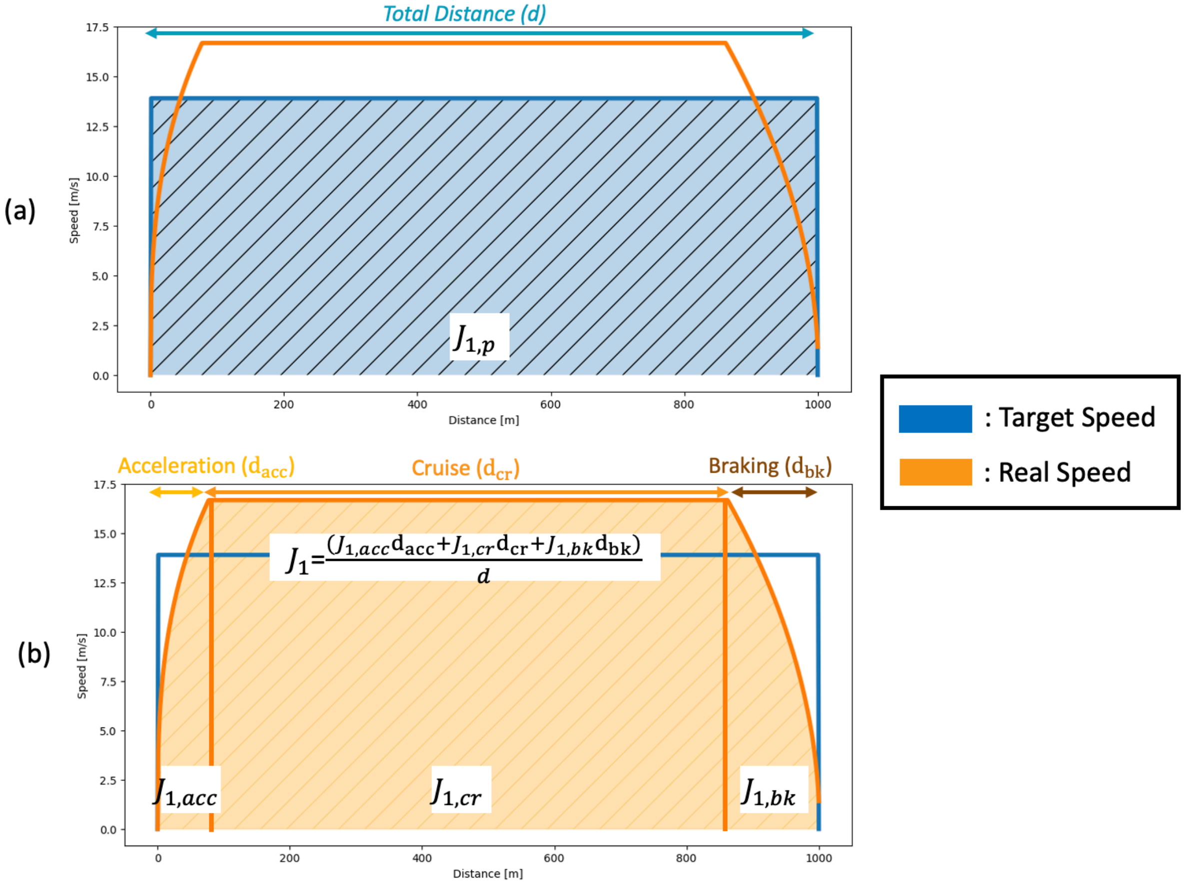

Figure S4: Graphical Representation of the speed integration (J_1). First (a), the rectangular target function (in blue) is integrated. The integral calculated is represented in hashed lines under the blue curb ($J_{1,p}$). Second (b), the real function (in orange) adapted from the target function is integrated with specific calculations for acceleration ($J_{1,ac}$), cruise ($J_{1,cr}$) and braking ($J_{1,bk}$). The hashed orange area represents the result of this calculation (J_1).

Since *target functions* are rectangular, they can be integrated manually by weighting the dynamic parameter values by the length of each segment (d_{sect}) .

For *real function* integration, separate calculations are done for cruising, acceleration, and deceleration. Assumptions A1 to A9 enable to model the impact of the driver behavior during these phases. As shown in section 2, acceleration, deceleration and cruising lengths are respectively $d_a = \frac{M(dK_2)}{P_a}$; $d_{bk} = \frac{dK_1}{B}$; $d_{cr} = d\left(1 - \frac{K_1}{B} - \frac{MK_2}{P_a}\right)$. These distances are used as weight coefficients to obtain the final dynamic variables integrals values (Figure S4b).

3.3.1) Vehicle Speed

For all J integrals (related to the speed) the following preparation is made based on the definition of speed $\mathrm{v} = \frac{\mathrm{dx}}{\mathrm{dt}}$.

$$For\ \alpha = (0,1,3),\ J_\alpha = \frac{1}{d}\int v^\alpha dt = \frac{1}{d}\int v^{\alpha-1}(vdt) = \frac{1}{d}\int v^{\alpha-1}dx \quad \text{(Equation S53)}$$

For the path target speed.
A constant speed $\mathrm{v_{path}}$ is assumed (A1). For a section, we obtain $\mathrm{J_{\alpha,sect}} = \mathrm{v_{path}^{\alpha-1}}$ and for the complete path, $\mathrm{J_{\alpha,p}} = \sum_{\mathrm{sect}} \frac{\mathrm{d_{sect}v_{path}^{\alpha-1}}}{\mathrm{d}}$.

For the real speed function.

For cruising, the speed is adapted to driver aggressiveness with $\mathrm{v_{sect}^{\alpha-1}}$=$(\mu_\mathrm{v}\mathrm{v_{path}})^{\alpha-1}$.
Thus, $\mathrm{J_{\alpha,cr}} = \frac{\mathrm{d_{cr}}}{\mathrm{d}}\sum_{\mathrm{sect}}\frac{\mathrm{d_{sect}v_{sect}}^{\alpha-1}}{\mathrm{d}} = \mu_\mathrm{v}^{\alpha-1}\mathrm{J_{\alpha,p}}(1 - \frac{\mathrm{K_1}}{\mathrm{B}} - \frac{\mathrm{MK_2}}{\mathrm{P_a}})$

For acceleration, the target speed is adjusted with the ratio $\mathrm{r_{acc}}$ calculated: $\mathrm{v_{acc}^{\alpha-1}} = (\mathrm{r_{acc}v_{sect}})^{\alpha-1}$. Thus, $\mathrm{J_{\alpha,acc}} = \mu_\mathrm{v}^{\alpha-1}\mathrm{r_{acc}^{\alpha-1}}\mathrm{J_{\alpha,p}}\frac{\mathrm{MK_2}}{\mathrm{P_a}}$

The braking phases are excluded from the integral bounds for GV. Thus, the integral is null during braking: $\mathrm{J_{\alpha,bk}} = 0$. For BEV, due to regenerative braking, the losses are evaluated during braking as all this energy dissipated will not be recovered by the regenerative system. Similarly, to acceleration, $\mathrm{J_{\alpha,bk}} = \mu_\mathrm{v}^{\alpha-1}\mathrm{r_{acc}^{\alpha-1}}\mathcal{J}_{\alpha,\mathrm{p}}\frac{\mathrm{K_1}}{\mathrm{B}}$.

These three terms are summed to obtain the final real speed integration (Eq. 54 and 55). Specific results for $\alpha = (0,1,3)$ are given in the table S5.

$$J_{\alpha,GV} = \mu_v^{\alpha-1}J_{\alpha,p}\left(1 - \frac{K_1}{B} - \frac{MK_2}{P_a}(1 - r_{acc}^{\alpha-1})\right) \quad \text{(Equation S54)}$$

$$J_{\alpha,BEV} = \mu_v^{\alpha-1}J_{\alpha,p}\left(1 - (\frac{K_1}{B} + \frac{MK_2}{P_a})(1 - r_{acc}^{\alpha-1})\right) \quad \text{(Equation S55)}$$

*Table S5: Equations used in the methodology to parametrize **the dynamic variables integrals linked to speed ($\boldsymbol{J_\alpha}$)**. The value for the target functions ($\boldsymbol{J_{\alpha,p}}$) and for the real functions for both GV and BEV are given.*

Var.	Target function	*Real function* for GV	*Real function* for BEV
$\boldsymbol{J_\alpha}$	$\sum_{sect} \frac{d_{sect} v_{path}^{\alpha-1}}{d}$	$J_{\alpha,GV} = \mu_v^{\alpha-1} J_{\alpha,p} \left(1 - \frac{K_1}{B} - \frac{MK_2}{P_a}(1 - r_{acc}^{\alpha-1})\right)$	$J_{\alpha,BEV} = \mu_v^{\alpha-1} J_{\alpha,p} \left(1 - (\frac{K_1}{B} + \frac{MK_2}{P_a})(1 - r_{acc}^{\alpha-1})\right)$
$\boldsymbol{J_1}$	1	$J_{1,GV} = \left(1 - \frac{K_1}{B}\right)$	$J_{1,BEV} = 1$
$\boldsymbol{J_3}$	$\sum_{sect} \frac{d_{sect} v_{path}^{2}}{d}$	$J_{3,GV} = \mu_v^2 J_{3,p} \left(1 - \frac{K_1}{B} - \frac{MK_2}{P_a}(1 - r_{acc}^2)\right)$	$J_{3,BEV} = \mu_v^2 J_{3,p} \left(1 - (\frac{K_1}{B} + \frac{MK_2}{P_a})(1 - r_{acc}^2)\right)$
$\boldsymbol{J_0}$	$\sum_{sect} \frac{d_{sect}}{d v_{path}}$	$J_{0,GV} = \frac{1}{\mu_v} J_{0,p} \left(1 - \frac{K_1}{B} - \frac{MK_2}{P_a}\left(1 - \frac{1}{r_{acc}}\right)\right)$	$J_{0,BEV} = \frac{1}{\mu_v} J_{0,p} \left(1 - (\frac{K_1}{B} + \frac{MK_2}{P_a})\left(1 - \frac{1}{r_{acc}}\right)\right)$

3.3.2) Engine Speed

For BEV, engine speed is proportional to speed based on (A4). Consequently, we obtain the equation S56 for calculating the integrals of the engine speed ($\mathcal{L}_{1,BEV}$) for BEV.

$\mathcal{L}_{1,BEV} = \sigma_{BEV} J_{1,BEV} = \sigma_{BEV}$ (Equation S56)

For GV, a distinction is made between cities, where the engine speed is constant (A5a) while on highway, the engine speed is proportional to speed (A5b). In both cases, the engine speed during acceleration phases is constant (A5c). The share of the distance traveled in urban area and in rural area are respectively given by the ratio r_{urban} and $r_{rural} = 1 - r_{urban}$. Following the same step than for vehicle speed integration, we obtain the table S6 which gathers the equation for the integrals linked to engine speed for GV.

Table S5: Equations used in the methodology to parametrize ***the dynamic variables integrals linked to engine speed for GV ($\mathcal{L}_\alpha$)****. The intermediary results for cruising ($\mathcal{L}_{\alpha,cr}$) and for the acceleration ($\mathcal{L}_{\alpha,acc}$) are also given. For cruising, a distinction between rural and urban paths is done.*

Var.	Urban	Rural
$\boldsymbol{\mathcal{L}_{1,cr}}$	$\mathcal{L}_{1,cr} = N_u J_{0,cr} = \frac{N_u}{\mu_v} J_{0,p}\left(1 - \frac{K_1}{B} - \frac{MK_2}{P_a}\right)$	$\mathcal{L}_{1,cr} = \sigma_r J_{1,cr} = \sigma_r\left(1 - \frac{K_1}{B} - \frac{MK_2}{P_a}\right)$
$\boldsymbol{\mathcal{L}_{1,acc}}$	$\mathcal{L}_{1,acc} = N_a J_{0,acc} = \frac{N_a t_a}{d} = \frac{N_a M K_1}{P_a}$	
$\boldsymbol{\mathcal{L}_{1,GV}}$	$\mathcal{L}_{1,GV} = r_{urban}\frac{N_u}{\mu_v} J_{0,p}\left(1 - \frac{K_1}{B} - \frac{MK_2}{P_a}\right) + r_{rural}\sigma_r\left(1 - \frac{K_1}{B} - \frac{MK_2}{P_a}\right) + \frac{N_a M K_1}{P_a}$	
$\boldsymbol{\mathcal{L}_{3,cr}}$	$\mathcal{L}_{3,cr} = \frac{N_u^3}{\mu_v} J_{0,p}\left(1 - \frac{K_1}{B} - \frac{MK_2}{P_a}\right)$	$\mathcal{L}_{3,cr} = \sigma_r \mu_v^2 J_{3,p}\left(1 - \frac{K_1}{B} - \frac{MK_2}{P_a}\right)$
$\boldsymbol{\mathcal{L}_{3,acc}}$	$\mathcal{L}_{3,acc} = \frac{N_a^3 M K_1}{P_a}$	
$\boldsymbol{\mathcal{L}_{3,GV}}$	$\mathcal{L}_{3,GV} = r_{urban}\frac{N_u^3}{\mu_v} J_{0,p}\left(1 - \frac{K_1}{B} - \frac{MK_2}{P_a}\right) + r_{rural}\sigma_r \mu_v^2 J_{3,p}\left(1 - \frac{K_1}{B} - \frac{MK_2}{P_a}\right) + \frac{N_a^3 M K_1}{P_a}$	

3.3.3) Engine Torque and Power for electric vehicles

It is assumed that the torque is negligeable during cruising and braking (A6). Moreover, a constant torque is assumed during acceleration $T_a = \sqrt{\mu_a} T_{max}$. Consequently, the equation S57 is obtained for the integral of the square torque ($\mathcal{T}_2$).

$\mathcal{T}_2 = \frac{1}{d}\int T^2\, dt = \frac{1}{d}\int_{acc} T_a^2\, dt = \frac{T_a^2 t_a}{d} = \frac{\mu_a T_{max}^2 M K_1}{P_a}$ (Equation S57)

Regarding power, power during acceleration is separated from the rest of power demand (A6). The power during acceleration corresponds to the power required for inertia, while the cruise power corresponds to the power required for all other losses. We assume that the two are decoupled.

$$\mathcal{P}_2 = \frac{1}{d}\int P^2\, dt = \frac{1}{d}\int (P_a^2 + P_{cruise}^2) dt = {P_a}^2 t_a/d + P_{cruise}^2 t/d$$

P_{cruise}^2 can be calculated using the overall energy consumption E_{cruise} over the travel expressed in J/m.

$$P_{cruise}^2 = (d.E_{cruise}/t)^{\,2}$$

Thus, we obtain the equation S58 characterizing the integral of the square power ($\mathcal{P}_2$).

$\mathcal{P}_2 = \frac{{P_a}^2 K_1 M}{P_a} + \frac{E_{cruise}^2 d}{t} = (\mu_a P_e K_1 M) + E_{cruise}^2/J_{0,el}$ (Equation S58)

3.3.4) Wind and Grade

Environmental parameters like grade and wind speed are averaged over the travel (A7). Based on this model, we obtain after calculations the equation S59 and S60.

$\mathcal{H} = \frac{1}{d}\int v sin\theta\, dt = \frac{1}{d}\int \frac{dx}{dt}\frac{dh}{dx}\, dt = \frac{H}{d} = h$ (Equation S59)

With H the total ascent climbed by the vehicle during the journey. In other words, h=H/d corresponds to the average slope of the road over the trip.

$W = \frac{1}{d}\int v v_{wind}^2\, dt = w^2 J_1$(Equation S60)

with w the average speed of the wind along the journey.

4- Parameters Influence on Energy Consumption (PIEC)

4.1 – General definition

For any parameter P of the model, the PIEC can be derived from the energy consumption equations for any automobile (both GV and BEV) as expressed in the Equation S60.

$PIEC = \frac{dEC}{dP}$ (Equation S60)

For instance, the Mass Influence on Energy Consumption (MIEC) is $MIEC = \frac{dEC}{dM}$ and the Drag Coefficient Influence on Energy Consumption (CdIEC) is $C_d IEC = \frac{dEC}{dC_d}$.

4.2 – Specific Case of the MIEC: secondary reduction

The specificity of the MIEC lies in the possible secondary effects due to the by reduction of the weight of the car[11,35] . The principal secondary effects modeled by the authors correspond to a reduction of the size of the engine. The main hypothesis of the authors is to consider that the power of the engine is proportional to the car weight.

The power of the engine can be decomposed with the maximal torque (T_{max}) and the engine speed (N_{max}) where the maximal power is reached following the Equation S61. As explained by Ross, the maximal torque is proportional to the engine displacement for GV (D). The engine speed of the engine is proportional to the gear ratio of the drivetrain (σ). Consequently, the power can be written as the third terms of the Equation S61, with x a proportional coefficient.

$P_e = T_{max} N_{max} = xD\sigma$ (Equation S61)

Consequently, two options can be explored for secondary reduction in lightweighting context: i- reducing the engine displacement (for GV)/ the maximum torque (for BEV); ii- reducing the gear ratio.

The associated secondary effects (MIEC_SR) to be added to the primary MIEC when considering a reduction of the engine displacement (Equation S62) and the gear ratio (Equation S63) proportional to mass reduction.

$MIEC_{SR} = \frac{D}{M}.DIEC$ (Equation S62)

$MIEC_{SR} = \frac{T_{max}}{M}.T_{max}IEC$ (Equation S62)

$MIEC_{SR} = \frac{\sigma_f}{M}.\sigma_f IEC$ (Equation S63)

It should be noted that the secondary reductions should be excluded from the LCA scope when the mass reduction from lightweight glazing is not significant enough[35].

Bibliography

1. Sovran. *A Contribution to Understanding Automotive Fuel Economy and Its Limits*. (2003).
2. Francesco Del Pero. *Tool for the Environmental Assessment in the Automotive Context: Analysis of the Use Stage for Different Typologies of LCA Study*. (2015).
3. Fontaras, G. & Zacharof, N. *Report on VECTO Technology Simulation Capabilities and Future Outlook*. (2016).
4. Ross, M. Fuel efficiency and the physics of automobiles. *Contemp Phys* **38**, 381–394 (1997).
5. Sacchi, R., Bauer, C., Cox, B. & Mutel, C. When, where and how can the electrification of passenger cars reduce greenhouse gas emissions? *Renewable and Sustainable Energy Reviews* **162**, (2022).
6. Tran, T. B. *et al.* Wind Sensitivity of Electric Vehicle Energy Consumption and Influence on Range Prediction and Optimal Vehicle Routes. in *2023 IEEE International Conference on Mobility, Operations, Services and Technologies (MOST)* 112–123 (IEEE, 2023). doi:10.1109/MOST57249.2023.00020.
7. Swift, A. Calculation of vehicle aerodynamic drag coefficients from velocity fitting of coastdown data. *Journal of Wind Engineering and Industrial Aerodynamics* **37**, 167–185 (1991).
8. Miri, I., Fotouhi, A. & Ewin, N. Electric vehicle energy consumption modelling and estimation—A case study. *Int J Energy Res* **45**, 501–520 (2021).
9. Zemansky, M. W. & Dittman, R. H. *Heat and Thermodynamics*. (McGraw-Hill Books, New York, 1981).
10. Heywood, J. *Internal Combustion Engine Fundamentals, 2nd Edition*. (McGraw Hill Education, 1988).
11. Kim, H. C. & Wallington, T. J. Life cycle assessment of vehicle lightweighting: A physics-based model of mass-induced fuel consumption. *Environ Sci Technol* **47**, 14358–14366 (2013).
12. Muranaka, S., Tagaki, Y. & Ishida, T. Factors Limiting the Improvement in Thermal Efficiency of S. I. Engine at Higher Compression Ratio. *SAE Transactions* **96**, 526–536 (1987).
13. Yagi, S., Fujiwara, K., Kuroki, N. & Maeda, Y. Estimate of Total Engine Loss and Engine Output in Four Stroke S.I. Engines. *SAE Transactions* **100**, 530–541 (1991).
14. Sandoval, D. & Heywood, J. An Improved Friction Model for Spark-Ignition Engines. *SAE Transactions* **112**, 1041–1052 (2003).
15. EPA. *Fuel Economy Guide*. (2024).
16. Mahmoudi, A., Soong, W. L., Pellegrino, G. & Armando, E. Efficiency maps of electrical machines. in *2015 IEEE Energy Conversion Congress and Exposition (ECCE)* 2791–2799 (IEEE, 2015). doi:10.1109/ECCE.2015.7310051.
17. Roshandel, E., Mahmoudi, A., Kahourzade, S., Yazdani, A. & Shafiullah, G. Losses in Efficiency Maps of Electric Vehicles: An Overview. *Energies (Basel)* **14**, 7805 (2021).
18. Habermehl, C., Jacobs, G. & Neumann, S. A modeling method for gear transmission efficiency in transient operating conditions. *Mech Mach Theory* **153**, 103996 (2020).
19. Talbot, D., Kahraman, A., Li, S., Singh, A. & Xu, H. Development and Validation of an Automotive Axle Power Loss Model. *Tribology Transactions* **59**, 707–719 (2016).

20. KUNT, M. A. Analysis of The Effect of Different Gearbox/Transmission Types on Driveline Friction Losses by Means of Gt Suite Simulation Programme. *International Journal of Automotive Science and Technology* **5**, 271–280 (2021).
21. Lee, D., Rousseau, A. & Rask, E. Development and validation of the ford focus battery electric vehicle model. in *SAE Technical Papers* vol. 1 (SAE International, 2014).
22. Ottaviano, D. *Technical Assessment and Modeling of Lithium-Ion Batteries for Electric Vehicles*.
23. Grunditz, E. A. & Thiringer, T. Performance analysis of current BEVs based on a comprehensive review of specifications. *IEEE Transactions on Transportation Electrification* vol. 2 270–289 Preprint at https://doi.org/10.1109/TTE.2016.2571783 (2016).
24. Reick, B., Konzept, A., Kaufmann, A., Stetter, R. & Engelmann, D. Influence of Charging Losses on Energy Consumption and CO2 Emissions of Battery-Electric Vehicles. *Vehicles* **3**, 736–748 (2021).
25. Ruan, J., Walker, P. D., Watterson, P. A. & Zhang, N. The dynamic performance and economic benefit of a blended braking system in a multi-speed battery electric vehicle. *Appl Energy* **183**, 1240–1258 (2016).
26. Mammosser, D., Boisvert, M. & Micheau, P. Designing a set of efficient regenerative braking strategies with a performance index tool. *Proceedings of the Institution of Mechanical Engineers, Part D: Journal of Automobile Engineering* **228**, 1505–1515 (2014).
27. Cox, B., Bauer, C., Mendoza Beltran, A., van Vuuren, D. P. & Mutel, C. L. Life cycle environmental and cost comparison of current and future passenger cars under different energy scenarios. *Appl Energy* **269**, 115021 (2020).
28. Rohde-Brandenburger, K. Verbrauch in Fahrzyklen und im Realverkehr. in *Energiemanagement im Kraftfahrzeug* 243–306 (Springer Fachmedien Wiesbaden, Wiesbaden, 2014). doi:10.1007/978-3-658-04451-0_7.
29. Qiu, C., Wang, G., Meng, M. & Shen, Y. A novel control strategy of regenerative braking system for electric vehicles under safety critical driving situations. *Energy* **149**, 329–340 (2018).
30. Kim, H. C. & Wallington, T. J. Life Cycle Assessment of Vehicle Lightweighting: A Physics-Based Model to Estimate Use-Phase Fuel Consumption of Electrified Vehicles. *Environ Sci Technol* **50**, 11226–11233 (2016).
31. Del Pero, F., Delogu, M. & Pierini, M. The effect of lightweighting in automotive LCA perspective: Estimation of mass-induced fuel consumption reduction for gasoline turbocharged vehicles. *J Clean Prod* **154**, 566–577 (2017).
32. Del Pero, F., Berzi, L., Antonacci, A. & Delogu, M. Automotive lightweight design: Simulation modeling of mass-related consumption for electric vehicles. *Machines* **8**, (2020).
33. Geyer, R. & Malen, D. E. Parsimonious powertrain modeling for environmental vehicle assessments: part 1—internal combustion vehicles. *Int J Life Cycle Assess* **25**, 1566–1575 (2020).
34. Geyer, R. & Malen, D. E. Parsimonious powertrain modeling for environmental vehicle assessments: part 2—electric vehicles. *International Journal of Life Cycle Assessment* **25**, 1576–1585 (2020).

35. Koffler, C. & Rohde-Brandenburger, K. On the calculation of fuel savings through lightweight design in automotive life cycle assessments. *International Journal of Life Cycle Assessment* **15**, 128–135 (2010).
36. Fiori, C., Ahn, K. & Rakha, H. A. Power-based electric vehicle energy consumption model: Model development and validation. *Appl Energy* **168**, 257–268 (2016).
37. Kneba, Z., Stepanenko, D. & Rudnicki, J. Numerical methodology for evaluation the combustion and emissions characteristics on WLTP in the light duty dual-fuel diesel vehicle. *Combustion Engines* **189**, 94–102 (2022).
38. Ben-Chaim, M., Shmerling, E. & Kuperman, A. Analytic Modeling of Vehicle Fuel Consumption. *Energies (Basel)* **6**, 117–127 (2013).
39. Sciarretta, A., De Nunzio, G. & Ojeda, L. L. Optimal Ecodriving Control: Energy-Efficient Driving of Road Vehicles as an Optimal Control Problem. *IEEE Control Syst* **35**, 71–90 (2015).